Article

Immunity

T-box Transcription Factors Combine with the Cytokines TGF-β and IL-15 to Control Tissue-Resident Memory T Cell Fate

Highlights

- $CD8^+CD103^+$ Trm cells protect against infection in the absence of circulating memory
- T-box transcription factor downregulation drives $CD8^+CD103^+$ Trm cell development
- TGF-β and the T-box transcription factors show reciprocal downregulation
- Residual T-bet expression is required for IL-15-mediated $CD8^+CD103^+$ Trm cell survival

Authors

Laura K. Mackay, Erica Wynne-Jones, David Freestone, ..., Axel Kallies, Gabrielle T. Belz, Francis R. Carbone

Correspondence

lkmackay@unimelb.edu.au

In Brief

Molecular events that regulate Trm cell formation remain poorly defined. Mackay and colleagues demonstrate that a complex interplay between Eomes and T-bet underpins $CD8^+CD103^+$ Trm cell formation. Although both T-box transcription factors must be downregulated, Eomes must be completely extinguished, whereas residual T-bet expression is essential for IL-15-mediated long-term survival.

Mackay et al., 2015, Immunity *43*, 1101–1111
December 15, 2015 ©2015 Elsevier Inc.
http://dx.doi.org/10.1016/j.immuni.2015.11.008

CellPress

Forte Biosciences, Inc. Exhibit - 1017
Forte Biosciences, Inc. v. University of Massachusetts - PGR2023-00014

Immunity
Article

T-box Transcription Factors Combine with the Cytokines TGF-β and IL-15 to Control Tissue-Resident Memory T Cell Fate

Laura K. Mackay,[1,*] Erica Wynne-Jones,[1] David Freestone,[1] Daniel G. Pellicci,[1,2] Lisa A. Mielke,[3] Dane M. Newman,[1] Asolina Braun,[1] Frederick Masson,[3,4,5] Axel Kallies,[3] Gabrielle T. Belz,[3,6] and Francis R. Carbone[1,6]
[1]Department of Microbiology and Immunology, The University of Melbourne, The Peter Doherty Institute for Infection and Immunity, Parkville, Victoria 3010, Australia
[2]Australian Research Council Centre of Excellence for Advanced Molecular Imaging, University of Melbourne, Parkville, Victoria 3010, Australia
[3]Walter and Eliza Hall Institute of Medical Research, Parkville, Victoria 3050, Australia
[4]Olivia Newton-John Cancer Research Institute, Heidelberg, Victoria 3084, Australia
[5]School of Cancer Medicine, La Trobe University, Melbourne, Victoria 3086, Australia
[6]Co-senior author
*Correspondence: lkmackay@unimelb.edu.au
http://dx.doi.org/10.1016/j.immuni.2015.11.008

SUMMARY

Tissue-resident memory T (Trm) cells contribute to local immune protection in non-lymphoid tissues such as skin and mucosa, but little is known about their transcriptional regulation. Here we showed that CD8$^+$CD103$^+$ Trm cells, independent of circulating memory T cells, were sufficient for protection against infection and described molecular elements that were crucial for their development in skin and lung. We demonstrated that the T-box transcription factors (TFs) Eomes and T-bet combined to control CD8$^+$CD103$^+$ Trm cell formation, such that their coordinate downregulation was crucial for TGF-β cytokine signaling. TGF-β signaling, in turn, resulted in reciprocal T-box TF downregulation. However, whereas extinguishment of Eomes was necessary for CD8$^+$CD103$^+$ Trm cell development, residual T-bet expression maintained cell surface interleukin-15 (IL-15) receptor β-chain (CD122) expression and thus IL-15 responsiveness. These findings indicate that the T-box TFs control the two cytokines, TGF-β and IL-15, which are pivotal for CD8$^+$CD103$^+$ Trm cell development and survival.

INTRODUCTION

Memory CD8$^+$ T cells in the blood have traditionally been classified as belonging to one of two subsets: central memory T (Tcm) cells that express the lymphoid homing markers CCR7 and CD62L, and effector memory T (Tem) cells that largely lack these receptors but instead express markers that allow them to enter peripheral tissues (Sallusto et al., 1999). When memory T cells were detected in the periphery, it was previously thought that these were Tem cells in transit through the body (Masopust et al., 2001; Reinhardt et al., 2001). However, more recent studies have determined that a proportion of T cells found in the tissues do not recirculate and instead represent a distinct population of tissue-resident memory T (Trm) cells. Initially described in detail in the skin (Gebhardt et al., 2009) and gut (Masopust et al., 2010), these cells have now been found in a variety of tissues and organs in both humans and mice (Casey et al., 2012; Sathaliyawala et al., 2013).

Trm cells often carry markers that are largely absent from memory cells in the circulation. Two such molecules are surface-expressed CD69 and CD103 (Mackay et al., 2013). CD69 is usually seen as an activation marker, but it can be upregulated in an antigen-independent fashion on T cells found in peripheral tissues (Casey et al., 2012; Mackay et al., 2013; Shin and Iwasaki, 2012). CD103, which is the integrin αEβ7, is driven by local transforming growth factor β (TGF-β) and its appearance is delayed in comparison to CD69 (Mackay et al., 2013). Although CD103 detection was originally used in the early analyses of Trm cell development and function (Gebhardt et al., 2009; Masopust et al., 2010), more recent discussions have focused on a broader Trm cell definition (Steinert et al., 2015; Thome et al., 2014; Watanabe et al., 2015). CD69 is found on the majority of Trm cells regardless of CD103 expression, and bona fide CD69$^+$ CD103$^-$ Trm cells have clearly been shown to exist (Steinert et al., 2015; Watanabe et al., 2015). However, given that CD69 is upregulated quite early in Trm cell development, at a time when tissue-egress mechanisms are not completely extinguished (Mackay et al., 2013; Skon et al., 2013), it remains possible that a fraction of T cells expressing this molecule can still return to the circulation. Thus, CD69 might not be a reliable marker of obligatory residency. This is particularly pertinent in the case of peripheral tissues such as skin, which contain a number of distinct resident and recirculating populations (Watanabe et al., 2015). In addition, Trm cell activation can promote recruitment of cells from the circulation (Schenkel et al., 2013), complicating the relative contribution of resident and recirculating T cells to overall peripheral immune control.

In contrast to this uncertainty regarding CD69$^+$ Trm cells, the CD103$^+$ subset of CD8$^+$ Trm cells are likely to represent a truly resident population in a variety of critical locations. These cells

dominate the epithelia of the small intestine and skin, where they remain in disequilibrium from the blood over the long term (Jiang et al., 2012; Klonowski et al., 2004). Such surfaces are common pathogen entry points in the body, indicating that the intra-epithelial CD8$^+$CD103$^+$ Trm cells might provide the first line-defense against many infectious agents. The CD8$^+$CD103$^+$ Trm cells are transcriptionally distinct from their CD103 negative tissue counterparts (Bergsbaken and Bevan, 2015; Wakim et al., 2012), as well as from Tem and Tcm cells in the circulation (Mackay et al., 2013). It has been shown that CD103 induction requires either local antigen recognition by Trm cells or their specific localization within the tissue (Mackay et al., 2012; Wakim et al., 2010), arguing that CD103$^+$ Trm cells likely represent late-stage tissue residents (Mackay et al., 2013).

One common feature of the mature CD8$^+$CD103$^+$ Trm cells in a range of different tissues is the near-extinguishment of Eomesodermin (Eomes) (Mackay et al., 2013; Wakim et al., 2012). Eomes is a T-box transcription factor (TF), which, along with the related homolog T-bet, is a major player in shaping the development of a range of cells belonging to the innate and adaptive arms of the immune system (Kaech and Cui, 2012). Eomes expression is upregulated in long-lived memory cells, whereas T-bet expression is highest in short-lived effector cells (Joshi et al., 2007). In terms of tissue T cells, it is known that T-bet downregulation is required for optimal CD8$^+$CD103$^+$ Trm cell development or survival in the lung (Laidlaw et al., 2014). However, T-bet and Eomes share cooperative functions (Banerjee et al., 2010; Intlekofer et al., 2005; Pearce et al., 2003), indicating that Eomes modulation might also play an equally important role in Trm cell formation.

Here we examined how the combination of T-bet and Eomes controlled Trm cell development, focusing on CD8$^+$CD103$^+$ Trm cells, which we showed had stand-alone protective capabilities in the absence of any contribution from the circulation. We further showed that the coordinated downregulation of both T-box TFs was required for optimal TGF-β signaling, leading to efficient CD8$^+$CD103$^+$ Trm cell development. However, while Eomes was effectively extinguished during Trm cell development, there was residual T-bet expression. The latter promoted interleukin-15 receptor (IL-15R) β-chain (CD122) expression and was required for long-term Trm cell survival. Therefore, while Trm cell development required the downregulation of both T-box TFs, the contribution of T-bet was distinct in that ongoing low-level expression of this TF was necessary to maintain IL-15 signaling and CD8$^+$CD103$^+$ Trm cell development and survival.

RESULTS

CD8$^+$CD103$^+$ Trm Cells Protect Skin against Herpes Simplex Virus Infection in the Absence of Circulating Memory T Cell Contribution

Trm cells can recruit memory T cells from the blood (Schenkel et al., 2013), which leaves open the possibility that Trm cell-mediated protection is completely dependent on the presence of circulating T cells. We wanted to see whether CD8$^+$ Trm cells alone could control infection in the absence of input from the circulating memory pool. To do this, we took advantage of the observation that systemic treatment with depleting antibodies eliminates circulating T cells, including memory cells,

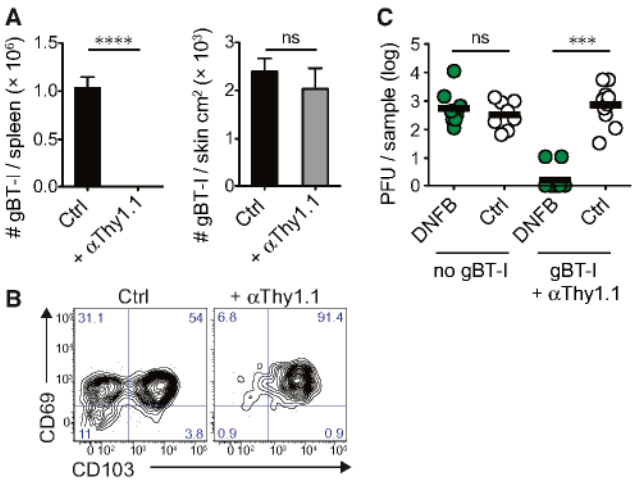

Figure 1. CD8$^+$CD103$^+$ Trm Cells Protect against Infection with HSV in the Absence of Circulating Memory

Mice were seeded with in vitro activated gBT-I.Thy1.1$^+$ T cells and treated with DNFB on one skin flank to lodge Trm cells. At > 30 days post DNFB treatment, mice (as indicated) were treated with anti-Thy1.1 antibody to deplete circulating Thy1.1$^+$ cells.

(A) Enumeration of gBT-I T cells in spleen and skin (CD103$^+$ Trm cells) and (B) co-expression of CD103 and CD69 by gBT-I T cells in skin, in antibody treated (+ αThy1.1) and non-treated (Ctrl) cohorts, at 7 days post antibody treatment. (C) Cohorts of mice that received gBT-I.Thy1.1$^+$ T cells and were treated with depleting antibody (gBT-I + Thy1.1) or that did not receive gBT-I T cells (no gBT-I) were infected with HSV on both DNFB-treated ("DNFB," green circles) and non-treated ("Ctrl," open circles) skin flanks > 30 days post DNFB-treatment and 7 days post antibody treatment. Shown are viral titers in the skin 6 days after HSV infection in the described cohorts. Symbols represent individual mice; bars represent the mean. Data are pooled from two experiments. Error bars represent mean ± SEM.

while leaving peripheral populations largely intact (Schenkel et al., 2013). To this end, we adoptively transferred in vitro-activated congenically marked Thy1.1$^+$ transgenic (gBT-I) T cells specific for the immunodominant determinant from herpes simplex virus (HSV) and then recruited them into the skin of C57BL/6 recipient mice via the induction of a local non-specific inflammatory reaction using the contact sensitizer DNFB, as previously described (Mackay et al., 2012). Intravenous administration of anti-Thy1.1 antibody was then used to eliminate all circulating HSV-specific T cells, including gBT-I T cells in the spleen, while sparing the Trm cell counterparts in the skin (Figure 1A). At the time of treatment (4 weeks after DNFB induced Trm cell lodgement), around 30% of skin gBT-I T cells were negative for CD103 and a high proportion of these expressed CD69 (Figure 1B). The anti-Thy1.1 antibody selectively eliminated all cells lacking CD103, which included a fraction of cells that expressed only CD69. There was virtually no loss of CD103$^+$ gBT-I T cells, defining them as separate from the circulation and thus true resident cells. To examine the functional capabilities of CD8$^+$CD103$^+$ Trm cells, we then challenged antibody-ablated and control mice with HSV on the left (DNFB treated) flank that contained the Trm cells (in the gBT-I group) and right flank lacking this population (Ctrl). The presence of infectious virus was assessed 6 days later. The results in Figure 1C show that CD103$^+$ Trm cells effectively

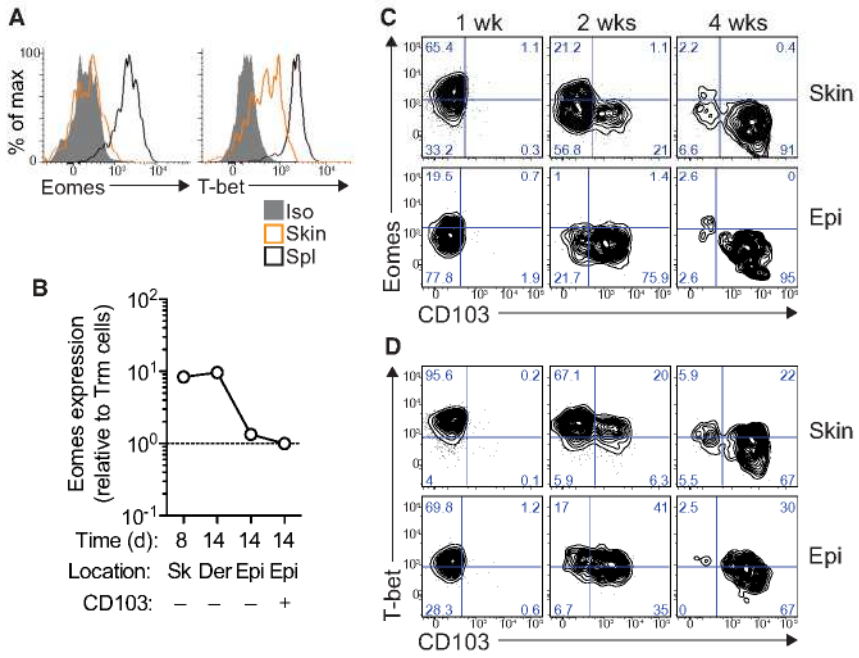

Figure 2. Expression of T-box Transcription Factors during Trm Cell Maturation in Skin

Mice received naive congenically marked gBT-I T cells and were infected on the flank with HSV. gBT-I T cells were tracked throughout the response based on their expression of Vα2, CD45.2, and CD45.1.

(A) Intracellular staining for Eomes and T-bet expression by gBT-I T cells in skin (orange line) and spleen (black line) > 4 weeks p.i. Isotype control staining is also shown (gray filled line).

(B) gBT-I T cells from skin 8 days and 14 days p.i. were sorted as indicated (Sk, total skin; Der, dermis; Epi, epidermis). Shown is qPCR analysis of Eomes expression during Trm cell differentiation. Median values were calculated relative to *Hprt* and normalized to Trm cell values. Data are pooled from three experiments (n = 15).

(C) Expression of Eomes and CD103 or (D) T-bet and CD103 by gBT-I T cells in skin and epidermis (Epi) at the indicated times p.i.; numbers depict percent events in respective gates. Data are representative of three experiments.

controlled local HSV replication in the absence of the circulating populations. Combined, these results define the CD103$^+$ subset of CD8$^+$ Trm cells as a true tissue-resident population that can directly protect skin against HSV challenge in the absence of circulating antigen-specific memory T cells.

T-box Transcription Factors Are Downregulated during CD8$^+$CD103$^+$ Trm Cell Maturation with Complete Shut-Down of Eomes Expression

We had previously carried out a detailed comparison of genes differently regulated in memory T cells resident in a variety of tissues to identify a core transcriptional signature of the CD103$^+$ Trm cell population (Mackay et al., 2013). As part of this signature, we found that Eomes transcription was strikingly downregulated in CD8$^+$CD103$^+$ Trm cells compared to circulating Tem or Tcm populations. Because both T-box TFs Eomes and T-bet can influence memory T cell development (Kaech and Cui, 2012), we were interested in tracking their coordinated expression during Trm cell maturation. Figure 2A shows that skin memory gBT-I T cells had no detectable intracellular Eomes expression after the resolution of HSV replication, whereas their splenic counterparts were Eomes positive. At this time, T-bet expression was similarly downregulated in skin memory T cells, although less so than Eomes (Figure 2A).

One of the advantages of the HSV skin infection model is that the development of skin Trm cells and the acquisition of the mature CD103$^+$ phenotype occurs in a progressive fashion, from the time T cells enter the skin during the effector response, to their entry into the epidermal layer and finally their surface acquisition of CD103 (Mackay et al., 2013). This allows the fine delineation of the molecular changes that occur during Trm cell maturation, as it is easy to separate epidermis (consisting exclusively of epithelium) from the dermis (which is largely non-epithelium, except for the hair follicles). Quantitative PCR (qPCR) analysis showed that virus-specific T cells had high *Eomes* transcript levels just after infection was cleared from the skin at day 8 after inoculation (Figure 2B). Transcription of this gene was progressively extinguished as the T cells subsequently migrated from the dermis to the epidermis and then in the latter compartment, converted to the mature CD103$^+$ form. This Eomes shut-down in skin T cells was also evident at the protein level, as determined by flow cytometry (Figure 2C). At later times after the resolution of HSV skin infection, most gBT-I T cells localized to the epithelium, such that by 4 weeks after infection, the pattern of staining for whole skin and epidermis had coalesced (Figure 2C). T-bet protein levels also declined after HSV infection (Figure 2D), although not to the same extent as seen with Eomes. Overall, these results show that expression of both T-box TFs is downregulated during CD8$^+$ Trm cell development in the skin, with the lowest amounts found in the most mature CD103$^+$ subset in the epidermis.

Forced Expression of T-box Transcription Factors Inhibits Trm Cell Formation in the Skin Epidermis

The data suggested that T-box TF downregulation might be required for Trm cell formation. To formally prove this, we forced the expression of either Eomes or T-bet in maturing Trm cells. We had previously shown that activated CD8$^+$ T cells injected into mouse skin are able to migrate into the epidermis and form stable Trm cells (Mackay et al., 2013). This approach allowed us to test whether T cells transduced to express Eomes or T-bet using recombinant retrovirus would be compromised in their ability to migrate to the epidermis and acquire the mature CD103$^+$ Trm cell phenotype.

Infection with recombinant retroviruses resulted in approximately 60%–90% transformation of T cells as determined by GFP expression. The transduced cells had high levels of T-box TF expression compared to cells transduced with the control

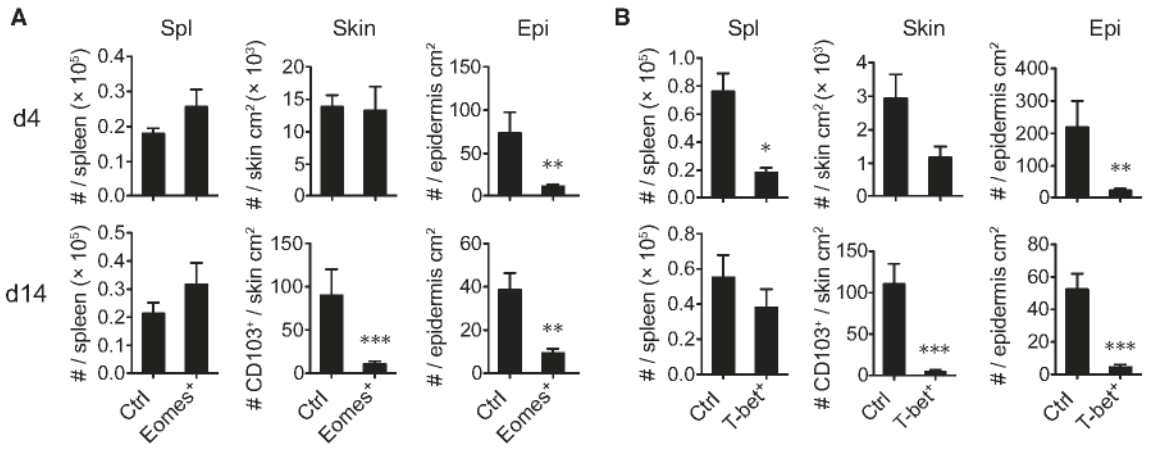

Figure 3. Forced Expression of T-box Transcription Factors Inhibits Trm Cell Formation in the Skin Epidermis

In vitro activated CD8$^+$ T cells were transduced with either control-GFP (Ctrl) retrovirus or (A) Eomes-GFP (Eomes$^+$), or (B) T-bet-GFP (T-bet$^+$) retrovirus. Equal numbers of GFP-expressing cells were injected intradermally into separate mice. Shown is the total number of GFP-expressing cells in the spleen (Spl), skin, and epidermis (Epi) at day 4 (upper panels), or the spleen and epidermis at days 14–17 (lower panels) post transfer. Note that following Trm cell maturation at > day 14, the number of CD103$^+$ Trm cells in skin is shown. Data are pooled from 2–3 experiments (n = 6–10 mice per group). Error bars represent mean ± SEM. See also Figure S1.

retrovirus (Figure S1A). Overexpression of either Eomes or T-bet did not change the expression of various surface markers such as CD44, Ly6C, and chemokine receptors CCR7 and CXCR6 (Figure S1B). In contrast, T cells transduced with the T-bet expression vector displayed higher levels of CD122 and CXCR3, both known to be induced by this TF (Matsuda et al., 2007), whereas the Eomes-containing vector resulted in a slight reduction in the latter molecule.

Retrovirus-transduced CD8$^+$ T cells were transferred by intradermal injection and identified in recipient mice as shown in Figure S1C. Some transferred cells were retained in the skin, while others made their way to the circulation and could be found in the spleen. Recovery of injected cells from the spleen was not affected by the forced Eomes expression, while there were far fewer Eomes-transduced T cells in the epidermal layer at either 4 or > 14 days after intradermal injection (Figure 3A) compared to cells transduced with control vectors. Thus, Eomes expression significantly inhibited CD103$^+$ Trm cell development (as detectable by day 14). Importantly, high T-bet expression had a similar effect, with T-bet transduced cells being severely compromised in their ability to form Trm cells in the epidermis (Figure 3B). Therefore, downregulation of T-box TF expression is required for epidermal entry and/or survival, and CD8$^+$CD103$^+$ Trm cell formation in skin.

T-box Transcription Factors and TGF-β Receptor Signaling Operate in a Feed-Forward Loop, Which Is Required for Efficient Trm Cell Formation in the Skin Epidermis

We and others have shown that TGF-β is required for Trm cell development in peripheral tissues such as the skin and gut, and that this cytokine drives the upregulation of the Trm cell markers CD103 and to a lesser extent CD69 (Casey et al., 2012; Mackay et al., 2013; Sheridan et al., 2014; Skon et al., 2013; Zhang and Bevan, 2013). Furthermore, it has been shown that TGF-β signals can negatively regulate T-bet expression in CD8$^+$ T cells (Laidlaw et al., 2014). We therefore wanted to determine when TGF-β signaling was required during Trm cell maturation, and whether this correlated with the downregulation of the other T-box TF Eomes, as well as T-bet. Wild-type OT-I T cells (specific for ovalbumin [OVA]) and TGF-βR deficient OT-I T cells (OT-I.*Tgfbr2*$^{f/f}$*Lck-Cre*; henceforth referred to as OTI.*Tgfbr2*$^{-/-}$) were transferred into mice that were subjected to infection with recombinant HSV expressing ovalbumin (HSV-OVA). As shown in Figure 4A, similar numbers of wild-type and TGF-βR deficient cells infiltrated infected skin early after infection. However, whereas wild-type cells upregulated CD103, the TGF-βR-deficient cells failed to do so (Figure 4B). OT-I T cells unable to respond to TGF-β signals were significantly impaired in their ability to enter and/or survive in the epidermal layer and were significantly reduced in number in this compartment compared to their wild-type counterparts after HSV infection (Figure 4A, right panel) or following in vitro activation and intradermal transfer (Figure S2A, right panel).

Not only were the TGF-βR deficient cells inefficient in epidermal entry and Trm cell formation, but they also expressed higher levels of both Eomes and T-bet in skin and epidermis (Figure 4C) demonstrating a role for TGF-β in downregulating the T-box TFs in these Trm cell-forming compartments. Note that Eomes and T-bet expression levels were unchanged on OT-I T cells in the circulation. In addition, we also found a reverse association between TGF-βR itself and T-box TFs. Retrovirus-transduced cells that expressed high levels of Eomes or T-bet showed depressed levels of TGF-βR expression (Figures 4D and S2B). In line with this, forced expression of these TFs resulted in an inability to respond to TGF-β signals, as detected by CD103 upregulation (Figures 4E and S2C). Moreover, following the transfer of Eomes and T-bet overexpressing cells into the skin, we found reduced expression of CD69 and the integrin CD49a (Figure S2D), which are Trm cell-associated molecules dependent on TGF-β signaling (Zhang and Bevan, 2013). It should be noted that CD103 is not expressed by T cells in

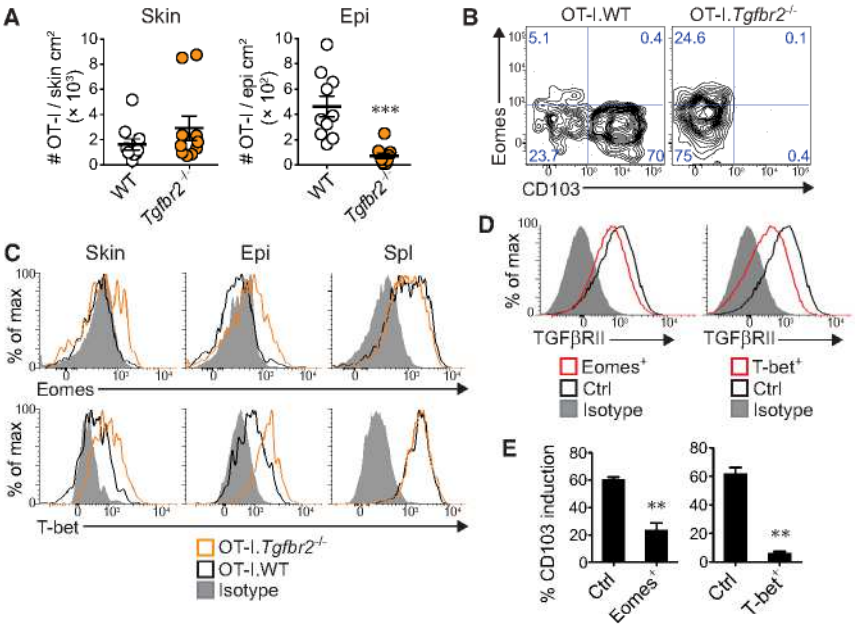

Figure 4. TGF-β Signaling and T-box Transcription Factor Regulation

(A–C) Mice received equal numbers of wild-type OT-I (WT) and OT-I.*Tgfbr2*$^{-/-}$ (*Tgfbr2*$^{-/-}$) T cells and were infected with HSV-OVA. (A) Shown is enumeration of OT-I T cells in skin and epidermis (Epi) 14 days p.i. Symbols represent individual mice. Data are pooled from two experiments (n = 10 mice/group). (B) Intracellular staining for Eomes and CD103 expression by OT-I T cells in skin at day 14 p.i.; numbers depict percent events in respective gates. (C) Histograms show expression levels of Eomes (upper panels) and T-bet (lower panels) by OT-I.WT (black line) or OT-I.*Tfbr2*$^{-/-}$ (orange line) T cells at 14d p.i. Data are representative of two experiments.

(D and E) In vitro activated CD8$^+$ T cells were transduced with either control-GFP (Ctrl) retrovirus or Eomes-GFP (Eomes$^+$) or T-bet-GFP (T-bet$^+$) retrovirus. (D) Representative histograms show expression of TGF-βRII levels by GFP-expressing cells, as indicated (72 hr post transduction). (E) Transduced cells were treated with TGF-β for 48 hr in vitro. Bar graphs show percent of CD103 induction. Data are representative of 2–3 experiments. Error bars represent mean ± SEM. See also Figure S2.

skin at early times after transfer (Figure S2D), and cells lacking this integrin subunit were not compromised in lodgement or survival for at least 14 days after transfer (Figure S2E). Combined, the data suggest that T-box TFs and the cytokine TGF-β operate in a feedforward loop during Trm cell development, where TGF-β drives the downregulation of the T-box TFs, which in turn promotes increased signaling via the cytokine receptor.

T-bet Elimination Results in Increased Proportion of KLRG1$^-$ Trm Cell Precursors and an Initially Greater Lodgement of CD8$^+$CD103$^+$ Trm Cells

Given that forced T-bet expression inhibited skin Trm cell formation, we wanted to determine whether its downregulation would promote early development of these memory cells. It should be noted that here we only focus on initial Trm cell lodgement (up to day 7), with longer-term survival examined in the next section. We began by using T cells homozygous or heterozygous for *Tbx21* (the gene encoding T-bet), which express lower amounts of T-bet. Although it has been reported that complete loss of T-bet results in increased Eomes expression (Takemoto et al., 2006), this is not the case for the OT-I T cells after HSV-OVA infection (Figure S3A). Thus, all changes in Eomes expression in skin memory *Tbx21*$^{-/-}$ T cells are likely to be a consequence of Trm cell maturation.

Low numbers of naive OT-I T cells that were either *Tbx21*$^{+/+}$ (wild-type) or *Tbx21*$^{+/-}$ (heterozygous) were transferred into recipient mice, and subsequently subjected to skin infection with HSV-OVA. At day 7 post infection, there was a modest increase in the number of CD103$^+$ Trm cells in skin for *Tbx21*$^{+/-}$ cells compared to their *Tbx21*$^{+/+}$ counterparts (Figure 5A, left panel). Although this difference did not reach statistical significance, the increase in Trm cell numbers should be viewed in the context of a significant decrease in overall splenic memory T cell numbers for *Tbx21*$^{+/-}$ cells (Figure 5A, middle

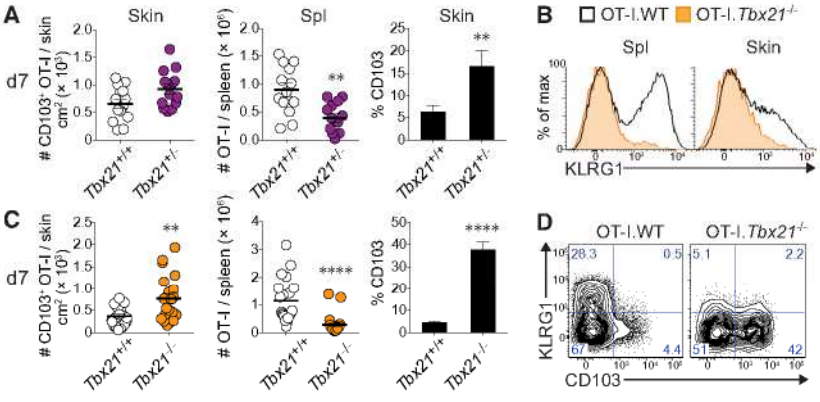

Figure 5. Enhanced Trm Cell Lodgment in the Absence of T-bet

Mice received equal numbers of wild-type OT-I (*Tbx21*$^{+/+}$) and (A) OT-I.*Tbx21*$^{+/-}$ or (B–D) OT-I.*Tbx21*$^{-/-}$ T cells and were infected with HSV-OVA. OT-I T cells were identified by Vα2 expression and distinct patterns of CD45.1 and CD45.2. (A) Shown is enumeration of OT-I (*Tbx21*$^{+/+}$) and OT-I.*Tbx21*$^{+/-}$ T cells in skin (CD103$^+$ Trm cells) and spleen (Spl) 7 days p.i. Bar graphs (right panel) show percent of OT-I T cells in skin that express the Trm cell marker CD103. (B) Plots show KLRG1 expression in the spleen and skin by OT-I.WT and OT-I.*Tbx21*$^{-/-}$ T cells 7 days p.i. (C) Enumeration of OT-I (*Tbx21*$^{+/+}$) and OT-I.*Tbx21*$^{-/-}$ T cells in skin (CD103$^+$ Trm cells) and spleen (Spl) 7 days p.i. Bar graphs as in (A).

(A and C) Symbols represent individual mice. Data are pooled from three experiments (n = 14–19 mice per group).

(D) KLRG1 and CD103 expression in skin by OT-I.WT and OT-I.*Tbx21*$^{-/-}$ T cells 7 days p.i. Data are representative of three experiments. Error bars represent mean ± SEM. See also Figure S3.

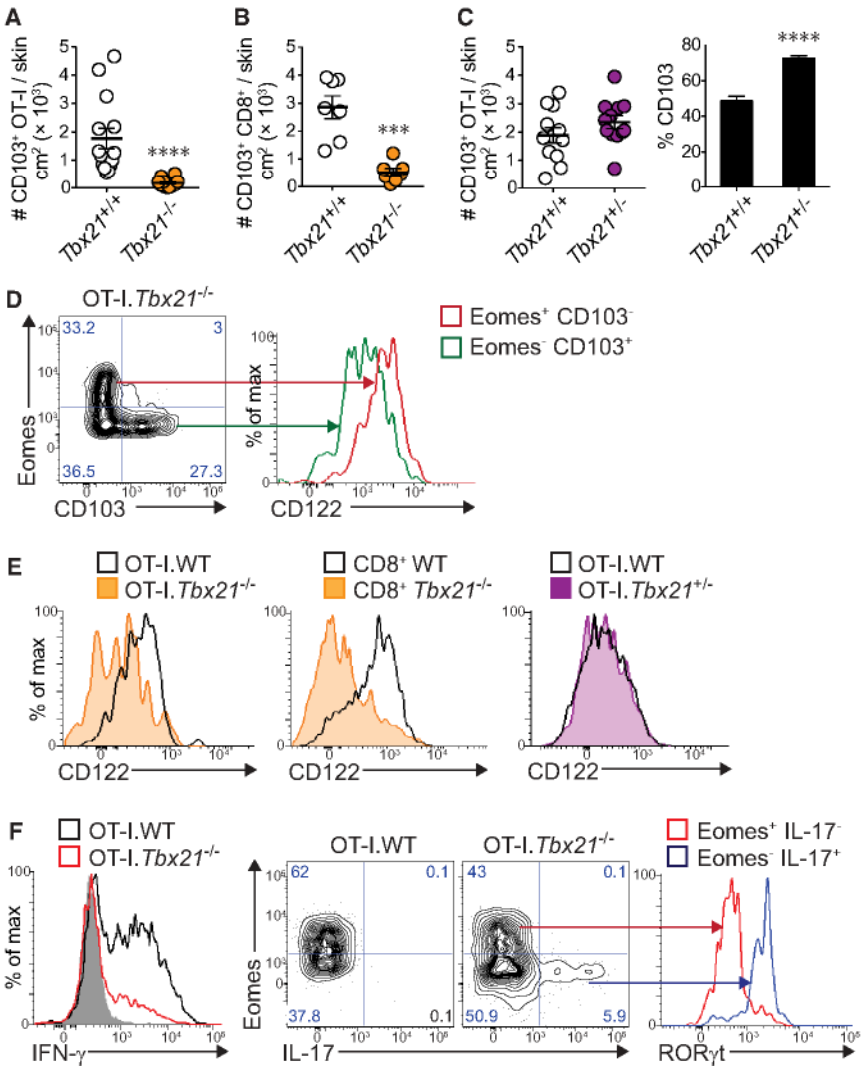

Figure 6. Defective Trm Cell Survival in the Absence of T-bet

(A) Mice received equal numbers of wild-type (WT) OT-I (*Tbx21*$^{+/+}$) and OT-I.*Tbx21*$^{-/-}$ (*Tbx21*$^{-/-}$) T cells and were infected with HSV-OVA. Shown is enumeration of OT-I T cells in skin (CD103$^+$ Trm cells) 14 days p.i.

(B) Mice received equal numbers of in vitro activated CD8$^+$ wild-type (*Tbx21*$^{+/+}$) and *Tbx21*$^{-/-}$ T cells by intradermal injection into skin. Shown is enumeration of CD8$^+$ T cells in skin (CD103$^+$ Trm cells) 14 days post transfer.

(C) Same as in (A) following co-transfer of WT OT-I (*Tbx21*$^{+/+}$) and OT-I.*Tbx21*$^{+/-}$ (*Tbx21*$^{+/-}$) T cells. Bar graphs (right panel) show percent of total OT-I T cells in skin that express the Trm cell marker CD103. Symbols represent individual mice. All data are pooled from 2–3 experiments (n = 11–17 mice/group). Error bars represent mean ± SEM.

(D) Intracellular staining for Eomes and CD103 expression by OT-I.*Tbx21*$^{-/-}$ T cells in skin at day 7 p.i. HSV-OVA; numbers depict percent events in respective gates. Histogram shows CD122 expression by Eomes$^+$ CD103$^-$ or Eomes$^-$ CD103$^+$ fractions, as indicated.

(E) Representative histograms show CD122 expression in skin (left panel) by OT-I.WT (black line) and OT-I.*Tbx21*$^{-/-}$ (orange filled) T cells 14 days p.i. HSV-OVA; (middle panel) by in vitro activated CD8$^+$ WT (black line) and CD8$^+$ *Tbx21*$^{-/-}$ (orange filled) T cells 14 days post intradermal transfer; and (right panel) by OT-I.WT (black line) and OT-I.*Tbx21*$^{+/-}$ (purple filled) T cells 14 days p.i. HSV-OVA.

(F) OT-I.WT and OT-I.*Tbx21*$^{-/-}$ T cells were isolated from the skin 7 days p.i. HSV-OVA and were stimulated for 4 hr in vitro with PMA and Ionomycin. Histogram (left panel) shows intracellular staining for IFN-γ by OT-I.WT (black line) OT-I.*Tbx21*$^{-/-}$ (red line) and non-stimulated T cells (gray filled). Contour plots show expression of Eomes and IL-17 by OT-I T cells as indicated; numbers depict percent events in respective gates. Histogram (right panel) shows RORγt expression by Eomes$^+$ IL-17$^-$ or Eomes$^-$ IL-17$^+$ OT-I.*Tbx21*$^{-/-}$ T cells. Data are representative of two experiments. See also Figures S3–S5.

panel), the latter due to the requirement for T-bet to generate a complete short-lived effector cell pool following viral infection (Joshi et al., 2007). The proportion of total skin T cells expressing the mature CD103$^+$ Trm cell phenotype was significantly higher in the *Tbx21*$^{+/-}$ cells (Figure 5A, right panel). Thus, even a modest reduction in T-bet promoted Trm cell formation.

Given the above, we wanted to determine whether complete elimination of T-bet would also promote greater lodgement of Trm cell precursors in the skin. Wild-type *Tbx21*$^{+/+}$ or *Tbx21*$^{-/-}$ OT-I T cells were transferred into recipient mice, which were then infected with HSV-OVA. As expected, *Tbx21*$^{-/-}$ cells in both spleen and skin showed a preferential skewing toward cells with low KLRG-1 expression (Figure 5B), which are the precursors of Trm cells (Mackay et al., 2013). Consistent with this increased precursor frequency, T-bet-deficient T cells were recovered in significantly greater numbers from the skin at day 7 post infection compared to their wild-type counterparts. Furthermore, a larger proportion of T-bet-deficient cells expressed CD103 (Figure 5C, D). Thus, complete elimination of T-bet expression results in the preferential production of KLRG-1$^-$ memory cell precursors, with a concomitant increase in CD103$^+$ Trm cell lodgement early after the resolution of skin infection.

T-bet-Deficient Trm Cells Show Defective IL-15Rβ Expression and Aberrant Cytokine Production and Disappear from the Skin over Time

Despite the enhanced CD103$^+$ Trm cell formation by T-bet deficient OT-I T cells seen at day 7 post infection (Figure 5C), the vast majority of these cells were lost by day 14 from the skin (Figure 6A). T-bet deficient CD103$^+$ Trm cells remaining at day 14 after HSV infection showed lower Bcl-2 levels, suggesting that survival in these few cells was also likely to be compromised (Figure S4A). *Tbx21*$^{-/-}$ Trm cells could not be rescued by Eomes

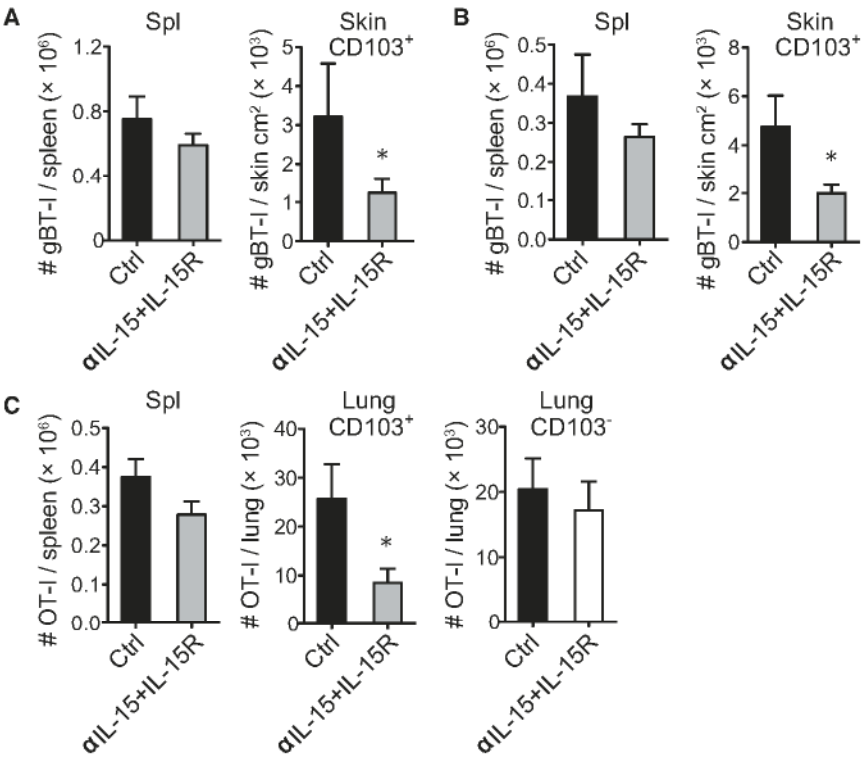

Figure 7. IL-15 Signaling Is Required for Initial Trm Cell Lodgment and Memory Trm Cell Survival

(A and B) Mice received naive gBT-I T cells and were infected on the flank with HSV. Mice were treated with αIL-15+IL-15R or PBS (Ctrl) by intradermal injection at the site of skin infection for 6 days (A) during Trm cell lodgment (days 7–13 p.i.) or (B) during the memory phase subsequent to Trm cell lodgment (> day 30 p.i.). Shown is enumeration of gBT-I T cells in spleen (Spl) and $CD103^+$ Trm cells in skin (n = 9–10 mice per group).

(**C**) Mice received naive OT-I T cells and were infected intranasally with X31-OVA. Mice were treated with αIL-15+IL-15R or PBS (Ctrl) by i.p. injection for 6 days > day 14 p.i. Shown is enumeration of OT-I T cells in the spleen (Spl) and $CD69^+CD103^+$ ($CD103^+$) and $CD69^+CD103^-$ ($CD103^-$) in the lung (n = 10 mice per group). Data are pooled from two experiments. Error bars represent mean ± SEM.

overexpression (Figure S4B), indicating that Eomes was either deleterious for Trm cell formation or that it simply could not efficiently substitute for T-bet in this particular subset. In contrast, T-bet deficient memory T cells in the circulation maintained Eomes expression (Figure S3A), unlike their $CD103^+$ counterparts in the skin that downregulate this TF as part of their maturation program (Figures 2 and S3B).

The preferential loss of T-bet-deficient Trm cells compared to their wild-type counterparts was also seen following injection of in vitro activated $CD8^+$ *Tbx21*$^{-/-}$ T cells directly into the skin (Figures 6B and S4C). Note that OT-I T cells heterozygous for T-bet were not lost from the skin, but instead were biased toward the $CD103^+$ Trm cell phenotype when compared to wild-type cells (Figure 6C). Thus, T-bet-deficient cells are lost over time despite their superior lodgement in skin early after infection. In contrast, Eomes deficiency was compatible with normal Trm cell development and maintenance in the skin (Figures S4D and S4E). These data established that the complete loss of T-bet, but not Eomes, was detrimental to long-term Trm cell survival.

T-bet-deficient $CD103^+$ Trm cells in the skin downregulated Eomes expression similar to their wild-type counterparts, effectively rendering them devoid of all T-box TF activity (Figure S3B). It has been reported that T cells lacking both Eomes and T-bet have defective expression of the β-chain (CD122) of the IL-15 receptor (Intlekofer et al., 2005). Given this, we hypothesized that impaired survival of T-bet deficient Trm cells was due to defective IL-15 signaling. In line with this idea, we found defective CD122 expression specifically in $CD103^+$ *Tbx21*$^{-/-}$ Trm cells that had downregulated Eomes early during maturation (Figure 6D). CD122 expression remained decreased on *Tbx21*$^{-/-}$ OT-I T cells (Figure 6E, left panel) and on in vitro stimulated *Tbx21*$^{-/-}$ $CD8^+$ T cells lodged by direct intradermal injection (Figure 6E, middle panel) even at later times clearly implicating impaired IL-15 signaling in the impaired survival of T-bet deficient Trm cells. In contrast, CD122 expression levels were equivalent between wild-type OT-I and OT-I.*Tbx21*$^{+/-}$ T cells (Figure 6E, right panel), which was consistent with their similar survival in skin.

In addition to the lack of CD122 expression, we found that T-bet deficient skin T cells that downregulated Eomes made less IFN-γ and secreted IL-17 with concomitant RORγt upregulation (Figure 6F). $CD8^+$ T cells deficient for both Eomes and T-bet have been shown to ectopically upregulate RORγt and IL-17 (Intlekofer et al., 2008), so the altered cytokine production was consistent with T-bet deficient skin T cells being effectively T-box TF negative once Eomes is downregulated. Thus, loss of T-bet has a profound effect on both Trm cell survival and the pattern of cytokine expression, which is likely linked to the downregulation of Eomes during the final stages of Trm cell development.

IL-15 Signaling Is Required for Ongoing Trm Cell Survival in Non-lymphoid Tissues

The concomitant failure in CD122 upregulation and Trm cell persistence of T-bet deficient T cells is consistent with the established role of IL-15 signaling in Trm cell development (Mackay et al., 2013). While Trm cell development was found to be impaired in IL-15 deficient mice, it was not clear whether the cytokine was just required for Trm cell formation or whether it also played a role in their subsequent survival. To address this, we administered neutralizing antibody specifically targeting the IL-15 and IL-15R complex. This antibody was injected into the skin flank at the site of Trm cell establishment, at two different periods following infection with HSV. We found that the number of skin Trm cells was diminished by more than half following antibody administration relatively early during the Trm cell formation phase (treatment day 7–13 post infection [p.i.] HSV, Figure 7A),

and also long after the Trm cell pool had been established (treatment > day 30 p.i. HSV, Figure 7B). Therefore, ongoing IL-15 signaling is required for skin Trm cell survival.

To extend our observation to another setting, we examined the IL-15 dependence of lung Trm cells. For these experiments, we transferred OT-I T cells into C57BL/6 mice and infected with recombinant influenza virus expressing the target determinant from ovalbumin (X31-OVA). Similar to $CD8^+CD103^+$ Trm cells in the skin, the corresponding subset in lungs showed downregulation of Eomes and T-bet expression (Figure S5A) with the decrease in Eomes and T-bet most pronounced in the mature $CD103^+$ population (Figures S5B and S5C). Moreover, similar to our results in the skin, T-bet elimination resulted in a pronounced loss of $CD8^+CD103^+$ Trm cells from the lung by day 14 after infection despite enhanced early lodgement (Figure S5D). Neutralization of the IL-15 and IL-15R complex by antibody injection showed that Trm cell survival in the lung was IL-15 dependent (Figure 7C). Interestingly, when we separately examined lung memory T cells based on their relative expression of CD103, only the $CD103^+$ T cells showed this reliance on IL-15 for ongoing survival (Figure 7C, right panel). Overall, the combined data suggest that skin and lung $CD8^+CD103^+$ Trm cells mirror each other in T-box TF requirements and, most critically, in their dependence on IL-15 signaling.

DISCUSSION

It is now emerging that Trm cells consist of different subsets, with varying expression of the markers CD69 and CD103 (Steinert et al., 2015; Watanabe et al., 2015). The $CD8^+CD103^+$ Trm cells form a transcriptionally distinct group (Wakim et al., 2012), which is found in a variety of different non-lymphoid organs, including the lung, skin, gut, and thymus (Casey et al., 2012; Hofmann et al., 2013; Hu et al., 2015; Mackay et al., 2013). In our study, we used antibody ablation to formalize two important characteristics for this population. First, we demonstrated that the $CD8^+CD103^+$ Trm cells have stand-alone protective capability. This is critical, because prior assessments of Trm cell-mediated protection were done in the presence of circulating memory cells (Mackay et al., 2012; Schenkel et al., 2014; Shin and Iwasaki, 2012), leaving open the possibility that infection control involved or even relied on recruitment from the blood. Separately, the experiments also showed that $CD8^+CD103^+$ skin T cells were truly resident, as distinct from a subset of skin T cells that only expressed CD69 and were eliminated by antibody depletion. While it has been shown that $CD69^+CD103^-$ T cells do not recirculate in some circumstances (Bergsbaken and Bevan, 2015; Steinert et al., 2015), our results argue that caution should be exercised when using CD69 as the sole Trm cell marker.

Having established the credentials for $CD8^+CD103^+$ Trm cells, we then focused on elucidating the role of the T-box TFs T-bet and Eomes during their development. While the importance of T-bet downregulation had been flagged by Laidlaw et al. (2014) for $CD8^+CD103^+$ Trm cells in the lung, those studies stopped short of examining the combined T-box TFs Eomes and T-bet as well as determining how they separately controlled Trm cell development. We found that, like T-bet, Eomes was also downregulated during Trm cell development, although to a much greater extent. Skin Trm cells virtually extinguish Eomes expression and do so quite late in the maturation program, either just before or just after the cells enter the epithelium and prior to the appearance of cell surface CD103. Leaving the matter of Eomes levels aside for the time being, the co-ordinated downregulation of both T-box TFs represents a pivotal step in Trm cell formation, since it was found to result in enhanced TGF-β signaling. This cytokine has been shown to be critical for $CD8^+CD103^+$ Trm cell development in a variety of tissues (Sheridan et al., 2014; Zhang and Bevan, 2013). We found that TGF-β signaling downregulated the T-box TFs, suggesting these both this cytokine and the T-box TFs are involved a feedforward loop that optimizes $CD8^+CD103^+$ Trm cell formation.

At face value, the earlier demonstration that T-bet modulation drove lung $CD8^+CD103^+$ Trm cell development (Laidlaw et al., 2014) implied that its complete elimination would have much the same effect. Initially, we found this to be the case, with T-bet deficient $CD8^+$ T cells showing early lodgement in the skin and acquisition of the mature $CD103^+$ phenotype. Moreover, the enhancement correlated with an increase in Trm cell precursor frequencies. T-bet deficiency favors development of $KLRG\text{-}1^-CD127^+$ memory precursor effector cells (MPECs) (Joshi et al., 2007), which are also the $CD8^+CD103^+$ Trm cell precursors (Mackay et al., 2013; Sheridan et al., 2014). In skin, KLRG-1- MPECs migrate into the epidermis after the resolution of HSV infection to form epidermal-lodged Trm cells (Mackay et al., 2013). In a related fashion, Sheridan et al. (2014) have shown that MPECs preferentially lodge in the intestinal mucosa after *Listeria monocytogenes* infection and, there, rapidly convert to $CD103^+$ Trm cells under the influence of local TGF-β stimulation.

However, despite exhibiting enhanced early lodgement in both skin and lung, the T-bet deficient $CD8^+CD103^+$ Trm cells were found to ultimately disappear over time. We propose that this disappearance is an indirect consequence of an effective lack of Eomes expression by the mature $CD8^+CD103^+$ Trm cells. Eomes shut-down is a striking feature that spans $CD8^+CD103^+$ Trm cells in a variety of different tissues including the skin and lung (Mackay et al., 2013; Wakim et al., 2012). This means that in cells that are genetically defective in *Tbx21*, *Eomes* extinguishment results in complete loss of T-box TF expression. Total T-box deficiency in $CD8^+$ T cells leads to altered functionality for this subset, with decreased IFN-γ production offset by the appearance of RORγt and IL-17 (Intlekofer et al., 2008). In line with this, we found that a proportion of T-bet deficient cells that downregulated Eomes could express RORγt and IL-17. More importantly, Intlekofer et al. (2005) also showed that at least one T-box TF was necessary to maintain expression of the cytokine receptor subunit CD122. As a consequence, skin T cells that genetically lacked T-bet and downregulated Eomes had little surface expression of the IL-15R β-chain. IL-15 is a prerequisite for Trm cell development (Mackay et al., 2013) and, as shown here in experiments using anti-IL-15 and IL-15R antibody blockade, it is also critical to the survival of Trm cells once lodged in the skin. Therefore, our results reveal a Trm cell-T-bet dependency that is linked to IL-15 signaling and set up by the loss of Eomes during the maturation process.

Putting the mechanisms described here in a broader context of tissue residency, the association between IL-15 and T-bet dependency for skin Trm cells mirrors what has been reported

for tissue-resident cells that form part of the innate system. Tissue-resident NK cells in skin and liver show similar patterns of low Eomes expression as well as IL-15 and T-bet-dependence (Sojka et al., 2014). In terms of other innate cells, CD8αα TCRαβ CD103$^+$ intra-epithelial lymphocytes (IELs) that reside in the intestinal mucosa appear to have a similar multifactorial dependence (Klose et al., 2014; Reis et al., 2014). These natural IELs are Eomes^{lo} and derive from distinct thymic T cell precursors that mature in the intestine in a TGF-β- and IL-15-dependent manner (Cheroutre et al., 2011). The IL-15 dependence for the CD8αα IELs is a consequence of T-bet driven CD122 expression (Reis et al., 2014), matching the results here for CD8$^+$CD103$^+$ Trm cells in both the skin and lung. Thus, some of the transcriptional regulations defined here for Trm cells are likely to be common to a variety of tissue-resident cells from both the innate and adaptive arms of the immune response.

In summary, our data reveal that both Eomes and T-bet are tightly regulated during Trm cell development and provide a critical interface with the cytokines TGF-β and IL-15. The Eomes extinguishment during the final stages of maturation renders skin CD8$^+$CD103$^+$ Trm cells completely T-bet dependent for their survival. One could envisage that under certain circumstances, elements involved in Trm cell development might be replaced by related factors, such as other cytokines that signal through of common γ-chain receptors acting as alternatives to IL-15. Given the complexity of this system and interdependence between the various components, changes that affect parameters such as the timing of T-box TF modulation and the coordination with TGF-β availability would also have a profound effect on Trm cell maturation. This, in turn, would directly affect the extent to which CD8$^+$CD103$^+$ Trm cells dominate the local response and mediate immunity within a given tissue. Understanding the various drivers of Trm cell development will permit optimization of their lodgement or survival for more effective immunity at pathogen entry points throughout the body.

EXPERIMENTAL PROCEDURES

Mice

C57BL/6, B6.SJL-PtprcaPep3b/BoyJ (B6.CD45.1), B6.Thy1.1, gBT-I, gBT-I.*Itgae*$^{-/-}$, OT-I, *Tbx21*$^{-/-}$, OT-I.*Tbx21*$^{-/-}$, OT-I.*Tbx21*$^{+/-}$, and OT-I.*Eomes*$^{-/-}$ mice were bred in the Department of Microbiology and Immunology, The University of Melbourne. Female mice 6–12 weeks of age were used for experiments. The gBT-I and OT-I mice are CD8$^+$ TCR transgenic mice that recognize the H-2K^b-restricted HSV-1 gB epitope of amino acids 498–505 ($gB_{498-505}$) and the ovalbumin-derived epitope of amino acids 257–264 ($OVA_{257-264}$), respectively. OT-I.*Tgfbr2*^{fl}.dLck-Cre mice were kindly provided by M. Bevan (University of Washington). All animal experiments were approved by The University of Melbourne Animal Ethics Committee.

Virus Infections and Determination of Viral Titers

Viruses used were the KOS strain of HSV-1 (HSV) and HSV-OVA (Mackay et al., 2013). Epicutaneous infection by scarification was carried out using 1 × 10^6 PFU HSV as described (Gebhardt et al., 2009). For influenza infections, 1 × 10^4 PFU X31-OVA (kindly provided by S. Turner) was administered intranasally. The level of infectious virus following HSV was determined within homogenized skin by standard PFU assays.

T Cell Transfers and In Vitro Activation

Adoptive transfers of naive gBT-I or OT-I T cells were carried out intravenously (i.v.) with lymph node suspensions. Naive gBT-I or OT-I T cells were transferred at a total number of 5 × 10^4 or 2.5 × 10^4 cells/population in co-transfer experiments, where cell types were transferred at a ratio of 1:1. For polyclonal in vitro activation of CD8$^+$ T cells, CD8-enriched splenocytes were activated by anti-CD3ε (145-2C11) and anti-CD28 (37.51) (5 μg/ml, eBioscience). For experiments where T cells were transferred by intradermal injection, 1–5 × 10^6 activated cells were transferred into recipients as described (Mackay et al., 2013). For experiments utilizing DNFB to lodge Trm cells for HSV challenge experiments, 1 × 10^7 gBT-I.Thy1.1$^+$ T cells were transferred i.v. and the skin flank was treated with 0.3% DNFB (Sigma-Aldrich), as described (Mackay et al., 2012).

Cytokine Treatments

For IL-15 blocking assays, mice were treated with anti-IL-15+IL-15R α chain antibody (7.5 μg/d, eBioscience) for 6 consecutive days by either intradermal injection (for experiments using HSV) or intraperitoneal injection (for experiments using influenza). For CD103 upregulation in vitro, CD8$^+$ T cells were treated for 48 hr with 5 ng/ml recombinant TGF-β. For depletion of circulating memory cells, mice were treated by intraperitoneal injection with 1 μg antibody to Thy1.1 (HIS51, BD Biosciences).

Retroviral Constructs and Transduction of CD8$^+$ T Cells

Murine stem cell virus (MSCV)–T-bet–internal ribosome entry site (IRES)–GFP has been previously described (Joshi et al., 2007), and MSCV-Eomes-IRES-GFP and MSCV-IRES-GFP were provided by Professor Gabrielle Belz (WEHI). In vitro activated CD8$^+$ T cells were spin-infected with retroviral supernatant 2d following activation in the presence of 1 μg/mL polybrene (Sigma-Aldrich) and 50 U/mL IL-2, and then expanded for a further 2–4 days in IL-2-containing medium. Transduction efficacy was determined by GFP expression and transduced cells (CD45.1$^+$) were transferred into C57BL/6 recipients by intradermal injection.

Flow Cytometry and Antibodies

T cells were recovered from skin as described (Mackay et al., 2012). Briefly, skin tissue was incubated for 90 min at 37°C in dispase (2.5mg/ml) followed by the separation of epidermis and dermis. Epidermal sheets were subsequently incubated for 30 min in trypsin/EDTA and remaining skin tissue was chopped into small fragments and incubated for 30 min at 37°C in collagenase type 3 (3 mg/ml). For recovery of T cells from the lung, mice were injected i.v. with 3 μg of Alexa Fluor 700-conjugated antibody to CD3 10 min prior to sacrifice, and mice were then perfused before the collection of lung tissue that was digested for 90 min in collagenase type 3 (3 mg/ml). Cell suspensions were stained with antibodies for flow cytometry. For intracellular staining, cells were fixed using Foxp3/Transcription Factor Staining Buffer Set (eBioscience) before staining with intracellular antibodies. For intracellular cytokine secretion assays, cells were incubated for 4 hr with PMA and Ionomycin in the presence of Brefeldin A. The following antibodies were purchased from BD PharMingen: anti-CD45.1 (A20), −CD45.2 (104), −Vα2 (B20.1), −CD8α (53-6.7), −TCR-β (H57-597), −Bcl-2 (3F11), and IL-17A (Tc11-18H10). The following antibodies were purchased from eBioscience: anti-CD45.1 (A20), −CD45.2 (104), −CD8α (53-6.7), −CD3 (500A2), anti-CD103 (2E7), −KLRG1 (2F1), CD122 (TM-b1), T-bet (4B10) Eomes (Dan11mag), and RORγt (AFKJS-9); anti-CXCR3 and -TGF-βRII were purchased from R&D.

qPCR

gBT-I T cells were isolated from skin and purified by cell sorting as PI$^-$Vα2$^+$ CD45.2$^+$CD45.1$^+$KLRG1$^-$CD103$^{+/-}$ events as indicated. RNA extraction, cDNA synthesis, preamplification and qPCR were performed using Taqman Gene Expression Cells-To-Ct Kit, Taqman Fast Preamp master mix and Taqman assays. The threshold cycle of respective genes for each cell population was normalized to the mean of Hprt, β2m, and Tbp (ΔCt). Normalized gene expression was compared to that of the Trm cell population according to the $2^{-\Delta\Delta CT}$ method.

Statistical Analysis

All statistics were calculated using the two-tailed Mann-Whitney test and GraphPad Prism (GraphPad Software). * $p < 0.05$, ** $p < 0.01$, *** $p < 0.001$, and **** $p < 0.0001$.

SUPPLEMENTAL INFORMATION

Supplemental Information includes five figures and can be found with this article online at http://dx.doi.org/10.1016/j.immuni.2015.11.008.

AUTHOR CONTRIBUTIONS

L.K.M. and F.R.C. designed the experiments; L.K.M., E.W.-J., D.F., D.G.P., L.A.M., D.M.N., and A.B. performed experiments; L.K.M., A.K., G.T.B., and F.R.C. analyzed and interpreted the data; F.M., A.K., and G.T.B. contributed reagents; L.K.M. and F.R.C. wrote the manuscript.

ACKNOWLEDGMENTS

We thank members of the Carbone and Heath laboratories for helpful discussions. We also thank J.M. Schenkel (University of Minnesota) for advice on Thy1.1 depletion and IL-15 blocking studies and S. Turner (University of Melbourne) for the influenza virus X31-OVA. This work was supported by National Health and Medical Research Council of Australia (L.K.M. and F.R.C.) and Australian Research Council (L.K.M. and F.R.C.).

Received: May 23, 2015
Revised: August 31, 2015
Accepted: September 14, 2015
Published: December 15, 2015

REFERENCES

Banerjee, A., Gordon, S.M., Intlekofer, A.M., Paley, M.A., Mooney, E.C., Lindsten, T., Wherry, E.J., and Reiner, S.L. (2010). Cutting edge: The transcription factor eomesodermin enables CD8+ T cells to compete for the memory cell niche. J. Immunol. *185*, 4988–4992.

Bergsbaken, T., and Bevan, M.J. (2015). Proinflammatory microenvironments within the intestine regulate the differentiation of tissue-resident CD8$^+$ T cells responding to infection. Nat. Immunol. *16*, 406–414.

Casey, K.A., Fraser, K.A., Schenkel, J.M., Moran, A., Abt, M.C., Beura, L.K., Lucas, P.J., Artis, D., Wherry, E.J., Hogquist, K., et al. (2012). Antigen-independent differentiation and maintenance of effector-like resident memory T cells in tissues. J. Immunol. *188*, 4866–4875.

Cheroutre, H., Lambolez, F., and Mucida, D. (2011). The light and dark sides of intestinal intraepithelial lymphocytes. Nat. Rev. Immunol. *11*, 445–456.

Gebhardt, T., Wakim, L.M., Eidsmo, L., Reading, P.C., Heath, W.R., and Carbone, F.R. (2009). Memory T cells in nonlymphoid tissue that provide enhanced local immunity during infection with herpes simplex virus. Nat. Immunol. *10*, 524–530.

Hofmann, M., Oschowitzer, A., Kurzhals, S.R., Krüger, C.C., and Pircher, H. (2013). Thymus-resident memory CD8+ T cells mediate local immunity. Eur. J. Immunol. *43*, 2295–2304.

Hu, Y., Lee, Y.T., Kaech, S.M., Garvy, B., and Cauley, L.S. (2015). Smad4 promotes differentiation of effector and circulating memory CD8 T cells but is dispensable for tissue-resident memory CD8 T cells. J. Immunol. *194*, 2407–2414.

Intlekofer, A.M., Takemoto, N., Wherry, E.J., Longworth, S.A., Northrup, J.T., Palanivel, V.R., Mullen, A.C., Gasink, C.R., Kaech, S.M., Miller, J.D., et al. (2005). Effector and memory CD8+ T cell fate coupled by T-bet and eomesodermin. Nat. Immunol. *6*, 1236–1244.

Intlekofer, A.M., Banerjee, A., Takemoto, N., Gordon, S.M., Dejong, C.S., Shin, H., Hunter, C.A., Wherry, E.J., Lindsten, T., and Reiner, S.L. (2008). Anomalous type 17 response to viral infection by CD8+ T cells lacking T-bet and eomesodermin. Science *321*, 408–411.

Jiang, X., Clark, R.A., Liu, L., Wagers, A.J., Fuhlbrigge, R.C., and Kupper, T.S. (2012). Skin infection generates non-migratory memory CD8+ T(RM) cells providing global skin immunity. Nature *483*, 227–231.

Joshi, N.S., Cui, W., Chandele, A., Lee, H.K., Urso, D.R., Hagman, J., Gapin, L., and Kaech, S.M. (2007). Inflammation directs memory precursor and short-lived effector CD8(+) T cell fates via the graded expression of T-bet transcription factor. Immunity *27*, 281–295.

Kaech, S.M., and Cui, W. (2012). Transcriptional control of effector and memory CD8+ T cell differentiation. Nat. Rev. Immunol. *12*, 749–761.

Klonowski, K.D., Williams, K.J., Marzo, A.L., Blair, D.A., Lingenheld, E.G., and Lefrançois, L. (2004). Dynamics of blood-borne CD8 memory T cell migration in vivo. Immunity *20*, 551–562.

Klose, C.S., Blatz, K., d'Hargues, Y., Hernandez, P.P., Kofoed-Nielsen, M., Ripka, J.F., Ebert, K., Arnold, S.J., Diefenbach, A., Palmer, E., and Tanriver, Y. (2014). The transcription factor T-bet is induced by IL-15 and thymic agonist selection and controls CD8$\alpha\alpha$(+) intraepithelial lymphocyte development. Immunity *41*, 230–243.

Laidlaw, B.J., Zhang, N., Marshall, H.D., Staron, M.M., Guan, T., Hu, Y., Cauley, L.S., Craft, J., and Kaech, S.M. (2014). CD4+ T cell help guides formation of CD103+ lung-resident memory CD8+ T cells during influenza viral infection. Immunity *41*, 633–645.

Mackay, L.K., Stock, A.T., Ma, J.Z., Jones, C.M., Kent, S.J., Mueller, S.N., Heath, W.R., Carbone, F.R., and Gebhardt, T. (2012). Long-lived epithelial immunity by tissue-resident memory T (TRM) cells in the absence of persisting local antigen presentation. Proc. Natl. Acad. Sci. USA *109*, 7037–7042.

Mackay, L.K., Rahimpour, A., Ma, J.Z., Collins, N., Stock, A.T., Hafon, M.L., Vega-Ramos, J., Lauzurica, P., Mueller, S.N., Stefanovic, T., et al. (2013). The developmental pathway for CD103(+)CD8+ tissue-resident memory T cells of skin. Nat. Immunol. *14*, 1294–1301.

Masopust, D., Vezys, V., Marzo, A.L., and Lefrançois, L. (2001). Preferential localization of effector memory cells in nonlymphoid tissue. Science *291*, 2413–2417.

Masopust, D., Choo, D., Vezys, V., Wherry, E.J., Duraiswamy, J., Akondy, R., Wang, J., Casey, K.A., Barber, D.L., Kawamura, K.S., et al. (2010). Dynamic T cell migration program provides resident memory within intestinal epithelium. J. Exp. Med. *207*, 553–564.

Matsuda, J.L., George, T.C., Hagman, J., and Gapin, L. (2007). Temporal dissection of T-bet functions. J. Immunol. *178*, 3457–3465.

Pearce, E.L., Mullen, A.C., Martins, G.A., Krawczyk, C.M., Hutchins, A.S., Zediak, V.P., Banica, M., DiCioccio, C.B., Gross, D.A., Mao, C.A., et al. (2003). Control of effector CD8+ T cell function by the transcription factor Eomesodermin. Science *302*, 1041–1043.

Reinhardt, R.L., Khoruts, A., Merica, R., Zell, T., and Jenkins, M.K. (2001). Visualizing the generation of memory CD4 T cells in the whole body. Nature *410*, 101–105.

Reis, B.S., Hoytema van Konijnenburg, D.P., Grivennikov, S.I., and Mucida, D. (2014). Transcription factor T-bet regulates intraepithelial lymphocyte functional maturation. Immunity *41*, 244–256.

Sallusto, F., Lenig, D., Förster, R., Lipp, M., and Lanzavecchia, A. (1999). Two subsets of memory T lymphocytes with distinct homing potentials and effector functions. Nature *401*, 708–712.

Sathaliyawala, T., Kubota, M., Yudanin, N., Turner, D., Camp, P., Thome, J.J., Bickham, K.L., Lerner, H., Goldstein, M., Sykes, M., et al. (2013). Distribution and compartmentalization of human circulating and tissue-resident memory T cell subsets. Immunity *38*, 187–197.

Schenkel, J.M., Fraser, K.A., Vezys, V., and Masopust, D. (2013). Sensing and alarm function of resident memory CD8$^+$ T cells. Nat. Immunol. *14*, 509–513.

Schenkel, J.M., Fraser, K.A., Beura, L.K., Pauken, K.E., Vezys, V., and Masopust, D. (2014). T cell memory. Resident memory CD8 T cells trigger protective innate and adaptive immune responses. Science *346*, 98–101.

Sheridan, B.S., Pham, Q.M., Lee, Y.T., Cauley, L.S., Puddington, L., and Lefrançois, L. (2014). Oral infection drives a distinct population of intestinal resident memory CD8(+) T cells with enhanced protective function. Immunity *40*, 747–757.

Shin, H., and Iwasaki, A. (2012). A vaccine strategy that protects against genital herpes by establishing local memory T cells. Nature *491*, 463–467.

Skon, C.N., Lee, J.Y., Anderson, K.G., Masopust, D., Hogquist, K.A., and Jameson, S.C. (2013). Transcriptional downregulation of S1pr1 is required

for the establishment of resident memory CD8+ T cells. Nat. Immunol. *14*, 1285–1293.

Sojka, D.K., Plougastel-Douglas, B., Yang, L., Pak-Wittel, M.A., Artyomov, M.N., Ivanova, Y., Zhong, C., Chase, J.M., Rothman, P.B., Yu, J., et al. (2014). Tissue-resident natural killer (NK) cells are cell lineages distinct from thymic and conventional splenic NK cells. eLife *3*, e01659.

Steinert, E.M., Schenkel, J.M., Fraser, K.A., Beura, L.K., Manlove, L.S., Igyártó, B.Z., Southern, P.J., and Masopust, D. (2015). Quantifying Memory CD8 T Cells Reveals Regionalization of Immunosurveillance. Cell *161*, 737–749.

Takemoto, N., Intlekofer, A.M., Northrup, J.T., Wherry, E.J., and Reiner, S.L. (2006). Cutting Edge: IL-12 inversely regulates T-bet and eomesodermin expression during pathogen-induced CD8+ T cell differentiation. J. Immunol. *177*, 7515–7519.

Thome, J.J., Yudanin, N., Ohmura, Y., Kubota, M., Grinshpun, B., Sathaliyawala, T., Kato, T., Lerner, H., Shen, Y., and Farber, D.L. (2014). Spatial map of human T cell compartmentalization and maintenance over decades of life. Cell *159*, 814–828.

Wakim, L.M., Woodward-Davis, A., and Bevan, M.J. (2010). Memory T cells persisting within the brain after local infection show functional adaptations to their tissue of residence. Proc. Natl. Acad. Sci. USA *107*, 17872–17879.

Wakim, L.M., Woodward-Davis, A., Liu, R., Hu, Y., Villadangos, J., Smyth, G., and Bevan, M.J. (2012). The molecular signature of tissue resident memory CD8 T cells isolated from the brain. J. Immunol. *189*, 3462–3471.

Watanabe, R., Gehad, A., Yang, C., Scott, L.L., Teague, J.E., Schlapbach, C., Elco, C.P., Huang, V., Matos, T.R., Kupper, T.S., and Clark, R.A. (2015). Human skin is protected by four functionally and phenotypically discrete populations of resident and recirculating memory T cells. Sci. Transl. Med. *7*, 279ra39.

Zhang, N., and Bevan, M.J. (2013). Transforming growth factor-β signaling controls the formation and maintenance of gut-resident memory T cells by regulating migration and retention. Immunity *39*, 687–696.

Immunity

Supplemental Information

T-box Transcription Factors Combine with the Cytokines TGF-β and IL-15 to Control Tissue-Resident Memory T Cell Fate

Laura K. Mackay, Erica Wynne-Jones, David Freestone, Daniel G. Pellicci, Lisa A. Mielke, Dane M. Newman, Asolina Braun, Frederick Masson, Axel Kallies, Gabrielle T. Belz, and Francis R. Carbone

Figure S1

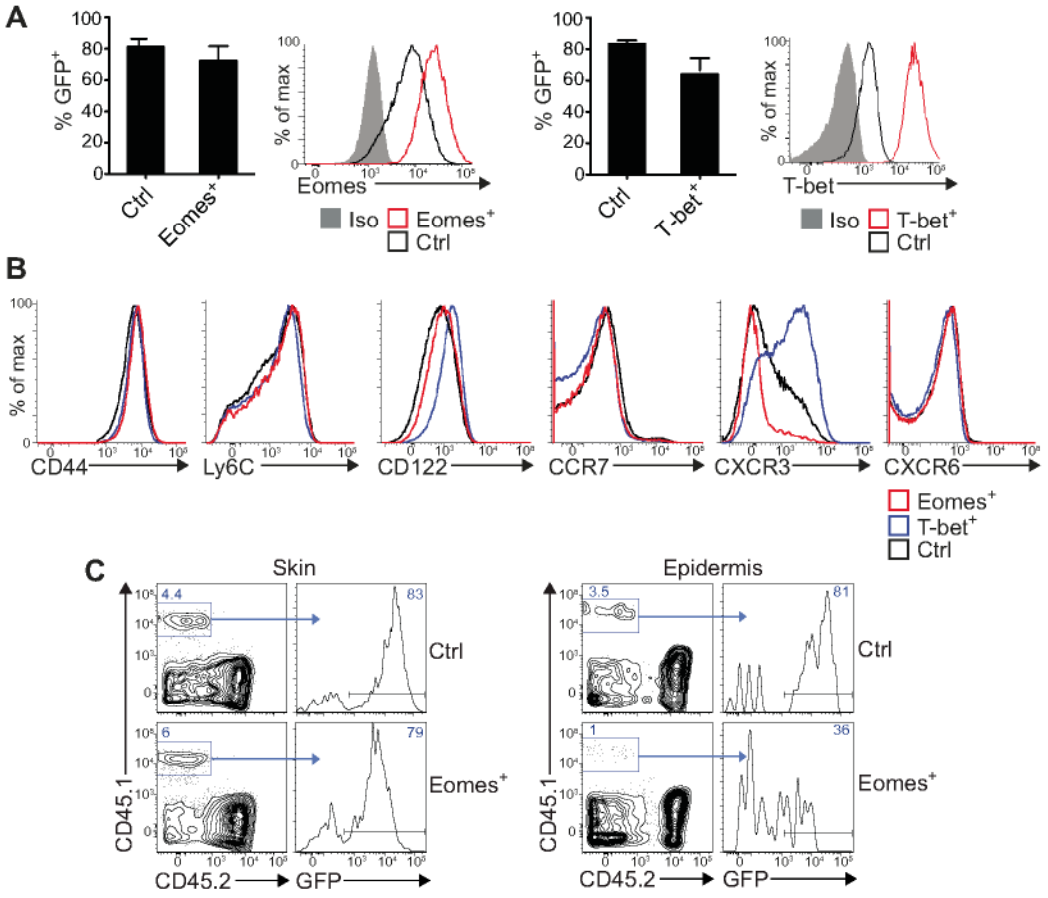
A
% GFP+
Ctrl
Eomes+
% of max
Eomes
Iso
Eomes+
Ctrl
T-bet+
T-bet
B
CD44
Ly6C
CD122
CCR7
CXCR3
CXCR6
C
Skin
Epidermis
4.4
83
6
79
3.5
81
1
36
CD45.1
CD45.2
GFP

Figure S2

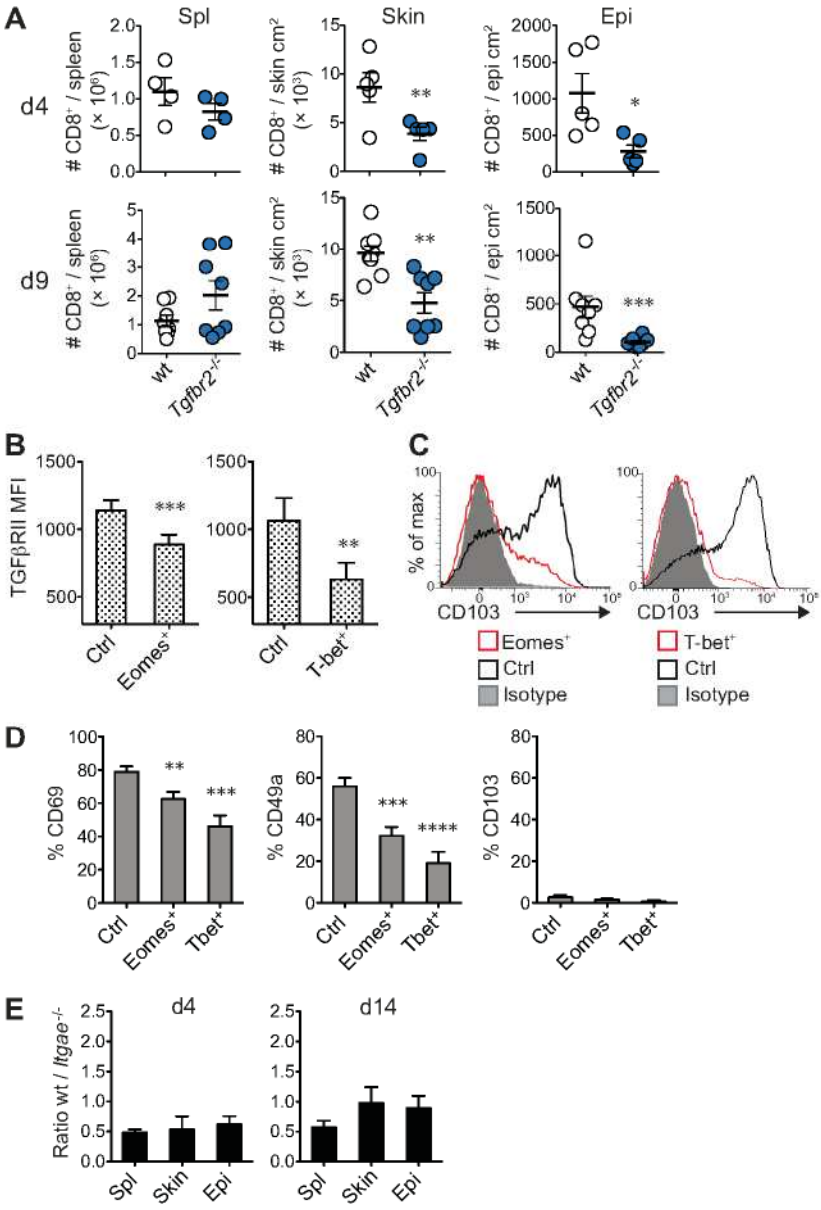
A
Spl
Skin
Epi
d4
d9
CD8+ / spleen (× 10^6)
CD8+ / skin cm2 (× 10^3)
CD8+ / epi cm2
wt
Tgfbr2-/-
B
TGFβRII MFI
Ctrl
Eomes+
T-bet+
C
% of max
CD103
Eomes+
T-bet+
Ctrl
Isotype
D
% CD69
% CD49a
% CD103
Ctrl
Eomes+
Tbet+
E
d4
d14
Ratio wt / Itgae-/-
Spl
Skin
Epi

Figure S3

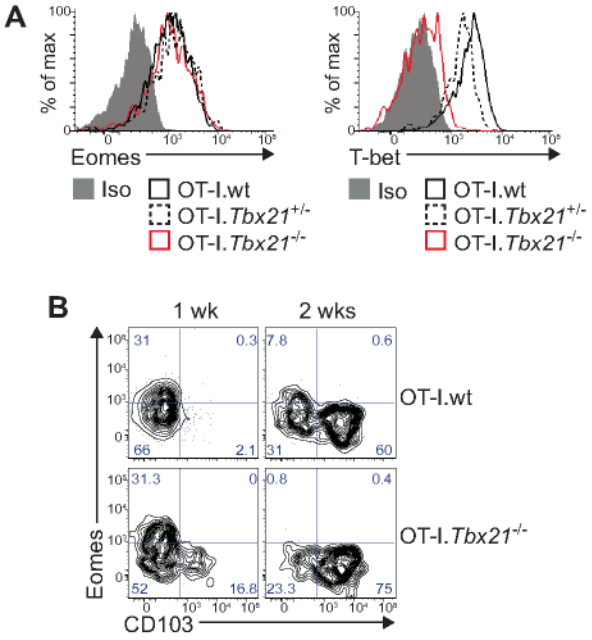
A
% of max
Eomes
T-bet
Iso
OT-I.wt
OT-I.Tbx21+/-
OT-I.Tbx21-/-
B
1 wk
2 wks
OT-I.wt
OT-I.Tbx21-/-
Eomes
CD103
31
0.3
66
2.1
7.8
0.6
31
60
31.3
0
52
16.8
0.8
0.4
23.3
75

Figure S4

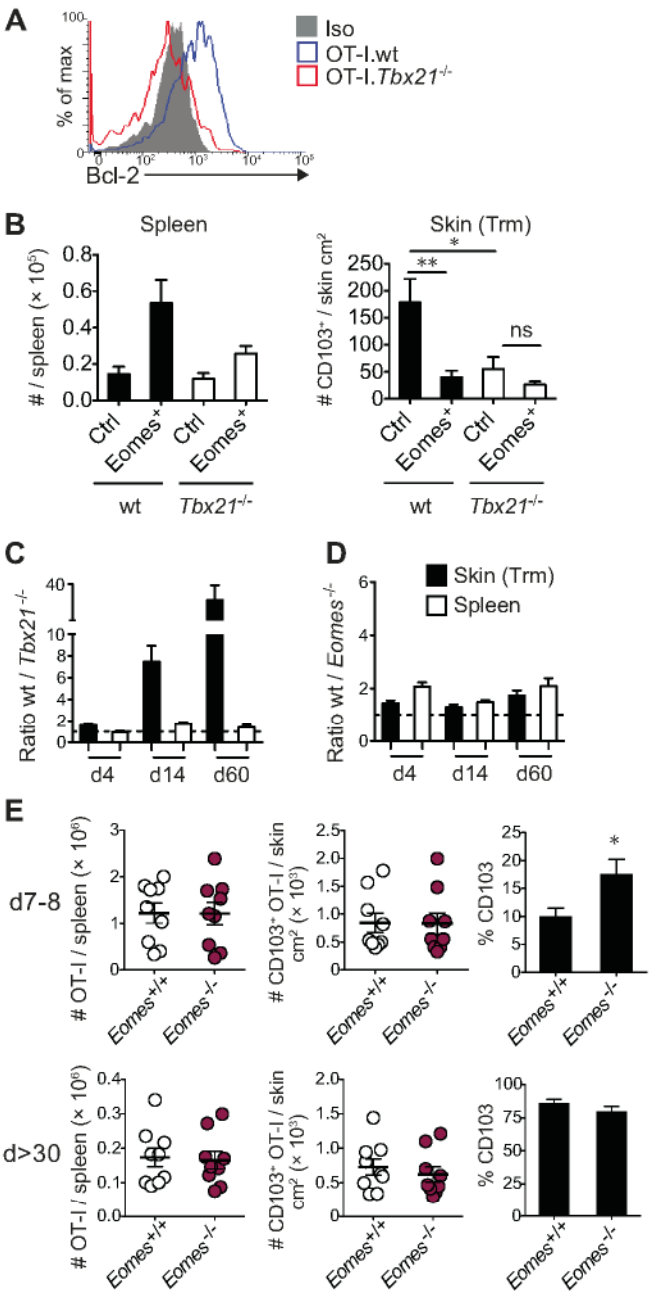
A
Iso
OT-I.wt
OT-I.Tbx21-/-
% of max
Bcl-2
B
Spleen
Skin (Trm)
/ spleen (× 10^5)
CD103+ / skin cm2
Ctrl
Eomes+
wt
Tbx21-/-
ns
C
Ratio wt / Tbx21-/-
d4
d14
d60
D
Skin (Trm)
Spleen
Ratio wt / Eomes-/-
E
d7-8
d>30
OT-I / spleen (× 10^6)
CD103+ OT-I / skin cm2 (× 10^3)
% CD103
Eomes+/+
Eomes-/-

Figure S5

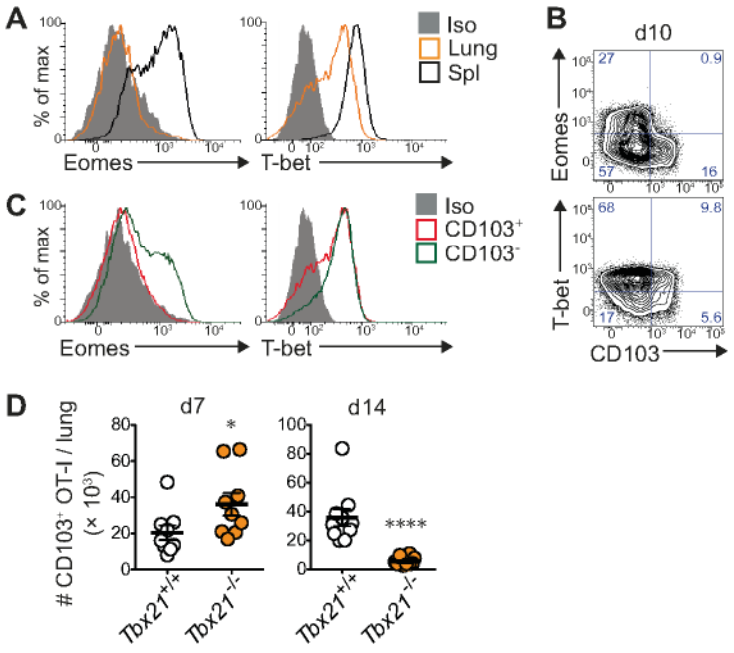
A
% of max
Iso
Lung
Spl
Eomes
T-bet
B
d10
Eomes
T-bet
CD103
27
0.9
57
16
68
9.8
17
5.6
C
% of max
Iso
CD103+
CD103-
Eomes
T-bet
D
d7
d14
CD103+ OT-I / lung (× 10³)
*
****
Tbx21+/+
Tbx21-/-

SUPPLEMENTAL FIGURE LEGENDS

Figure S1. Forced expression of T-box transcription factors by retroviral transduction of CD8⁺ T cells. Related to Figure 3. (A-C) *In vitro* activated CD8⁺ T cells were transduced with control-GFP (Ctrl), Eomes-GFP (Eomes⁺) or T-bet-GFP (T-bet⁺)-expressing retrovirus. (A) Bar graphs show the efficiency of transduction as measured by GFP expression and representative histograms show Eomes or T-bet expression from transduced CD8⁺ T cells (72h post-transduction), as indicated. Isotype control staining is also shown (gray filled line). Data is pooled from 2-3 experiments. (B) Histograms show surface expression of CD44, Ly6C, CD122, CCR7, CXCR3 and CXCR6 on transduced T cells *in vitro*, as indicated. (C) Gating strategy for detection of retrovirus-transduced T cells following transfer *in vivo*. Transduced CD8⁺ T cells (CD45.1⁺) were intradermally transferred into CD45.2⁺ recipients and were then identified as CD45.1⁺ GFP⁺ events. Shown are representative flow cytometry plots of CD8⁺ T cells transduced with control-GFP (Ctrl, upper panels) or Eomes-GFP (Eomes⁺, lower panels) retrovirus in the Skin and Epidermis 4d post transfer. Contour plots are gated on TCRβ⁺ CD3⁺ events and histograms are gated on CD45.1⁺ events, as indicated. Data is representative of >3 experiments.

Figure S2. TGF-β signaling and T-box transcription factor regulation. Related to Figure 4. (A) Equal numbers of *in vitro* activated CD8⁺ wild-type (wt) and *Tgfbr2*$^{-/-}$ T cells were injected intradermally into mice. Shown is enumeration of transferred CD8⁺ T cells in the spleen, skin and epidermis at the indicated times post transfer. Symbols represent individual mice (n = 4-8 mice/group). (B-D) *In vitro* activated CD8⁺ T cells were transduced with Eomes-GFP (Eomes⁺) or T-bet-GFP (T-bet⁺) retrovirus, or control-GFP (Ctrl) retrovirus. (B) Histograms show MFI of TGFβRII expression on GFP-expressing cells, as indicated. Data is pooled from 5 independent experiments. (C) Transduced cells were treated with TGF-β for 48h *in vitro*. Representative histograms show CD103 induction by transduced cells, as indicated. Isotype staining is also shown as indicated. Data is representative of 2-3 experiments. (D) Transduced cells were injected intradermally into mice. Shown is expression of CD69, CD49a and

CD103 on GFP-expressing cells in the skin at d4 post transfer (*n* = 9-13 mice/group). (E) Equal numbers of *in vitro* activated wild-type gBT-I (wt) and gBT-I.*Itgae*$^{-/-}$ (*Itgae*$^{-/-}$) T cells were injected intradermally into mice. Shown is the ratio of wt relative to *Itgae*$^{-/-}$ T cells in the spleen (Spl), skin and epidermis (Epi) at the indicated times post transfer (*n* = 5/group).

Figure S3. T-box transcription factor expression by transgenic OT-I T cells. Related to Figures 5 and 6. Equal numbers of wild-type (wt) and *Tbx21*$^{-/-}$ or *Tbx21*$^{+/-}$ OT-I T cells expressing distinct patterns of CD45.1 and CD45.2 were co-transferred into mice prior to HSV-OVA infection. (A) Intracellular staining for Eomes and T-bet expression by OT-I T cells in the spleen (gated on CD8$^+$ Vα2$^+$ cells) at d7 p.i. (B) Expression of Eomes and CD103 by OT-I.wt (upper panels) and OT-I.*Tbx21*$^{-/-}$ (lower panels) T cells in skin at the indicated times p.i.; numbers depict percent events in respective gates. Data is representative of 2 experiments.

Figure S4. T-bet deficient T cells, but not Eomes-deficient T cells show defective Trm cell development in skin. Related to Figure 6. (A) Mice received equal numbers of wild-type OT-I (OT-I.wt) and OT-I.*Tbx21*$^{-/-}$ T cells and were infected with HSV-OVA. Shown is intracellular staining for Bcl-2 expression by OT-I.wt (blue line) and OT-I.*Tbx21*$^{-/-}$ (red line) T cells in the skin 14d p.i HSV-OVA. (B) Equal numbers of *in vitro* activated wild-type (wt) and *Tbx21*$^{-/-}$ CD8$^+$ T cells were transduced with either control-GFP (Ctrl) retrovirus or Eomes-GFP (Eomes$^+$) retrovirus, and were injected intradermally into mice. Shown is the total number of GFP-expressing cells in the spleen (Spl, left panel) and CD103$^+$ Trm cells in the skin (right panel) at d14-16 post transfer. Data is pooled from 3 experiments (*n* = 10–17 mice/group). (C, D) Equal numbers of *in vitro* activated (C) wild-type (wt) and *Tbx21*$^{-/-}$ or (D) wt and *Eomes*$^{-/-}$ CD8$^+$ T cells were injected intradermally into mice. Shown is the ratio of wt relative to *Eomes*$^{-/-}$ CD8$^+$ T cells in the spleen and CD103$^+$ Trm cells in skin at the indicated times post transfer. Data is pooled from 2 experiments (*n* = 7–10 mice/group) in C, (*n* = 6–8 mice/group) in D. (E) Mice received equal numbers of wild-type OT-I (*Eomes*$^{+/+}$) and OT-I.*Eomes*$^{-/-}$ (*Eomes*$^{-/-}$) T cells and were infected with HSV-OVA. Shown is

enumeration of OT-I T cells in the spleen and CD103$^+$ Trm cells in skin at the indicated times p.i. Symbols represent individual mice. Bar graph (right panel) shows percent of total OT-I T cells in skin that express the Trm cell marker CD103. Data is pooled from 2 experiments (n = 9–10 mice/group).

Figure S5. Down-regulation of T-box transcription factors during lung Trm cell development and defective Trm cell survival in the complete absence of T-bet. Related to Figure 6. (A-D) Mice received naïve OT-I T cells and were infected intranasally with X31-OVA. Mice were injected i.v. with CD3 antibody prior to sacrifice to distinguish tissue-associated cells. OT-I T cells were tracked throughout the response based on their expression of Vα2, CD45.2 and CD45.1, and were gated as CD3 i.v. negative events in the lung. (A) Intracellular staining for Eomes and T-bet expression by OT-I T cells in the lung (orange line) and spleen (black line) 10d p.i. Isotype control staining is also shown (gray filled line). (B) Expression of CD103 and Eomes (upper panels) or T-bet (lower panels) by OT-I T cells in the lung at d10 p.i.; numbers depict percent events in respective gates. (C) Eomes and T-bet expression by CD103$^+$ (red line) and CD103$^-$ (green line) OT-I T cells in the lung 10d p.i. Isotype control staining is also shown (gray filled line). All Data (A-C) is concatenated from 5 mice and is representative of 3 experiments. (D) Mice received equal numbers of wild-type OT-I (*Tbx21*$^{+/+}$) and OT-I.*Tbx21*$^{-/-}$ (*Tbx21*$^{-/-}$) T cells and were infected with X31-OVA. Shown is enumeration of OT-I T cells in the lung (CD103$^+$ Trm cells) 7d and 14d p.i. Data is pooled from 2 experiments (n = 9-10 mice/group).